applied sciences

MDPI

Article

Effectiveness of Biomass Pellet Parameters on Their Fractal Dimension

Jianchao Zhang †, Xuehong De †, Zhihong Yu *, Wenbin Guo, Yan Ge and Xiaochao Chen

College of Mechanical and Electrical Engineering, Inner Mongolia Agricultural University, Hohhot 010018, China
* Correspondence: yzhyq@imau.edu.cn
† These authors contributed equally to this work.

Abstract: In order to perform quantitative analysis and predict the wear of the forming channel, this study makes biomass pellets as experimental samples. The surface morphology was scanned by a scanning electron microscope (SEM), and the surface morphology data and images were collected by a roughness instrument. Then, we collected the data of arithmetical average deviation *R*a, density ρ, as well as hardness HD, and further calculated the fractal dimension *D*, which help to study the influencing factors of fractal dimension on the circular surface morphology of biomass pellet. The results show that, the density ρ and hardness HD of biomass pellets both decreased and with the increase in diameter *d*, the arithmetical average deviation *R*a increased with the diameter *d*, the quality of the pellet is reduced, meanwhile, the fractal dimension *D* also shows a downward trend. Using the value, trend of fractal dimension *D* to analyze the quality of biomass pellet can predict the wear status and life of forming channel in biomass briquette machine. It is concluded that, the fractal expression of surface morphology in biomass pellet relates to inner surface morphology of forming channel in biomass pelleting machine. Additionally, fractal dimension of the surface morphology of biomass pellet can be the basis of preliminary research for friction and wear detection and prediction of forming channel.

Keywords: biomass; pellet; fractal dimension; arithmetical average deviation (*R*a)

check for updates

Citation: Zhang, J.; De, X.; Yu, Z.; Guo, W.; Ge, Y.; Chen, X. Effectiveness of Biomass Pellet Parameters on Their Fractal Dimension. *Appl. Sci.* **2022**, *12*, 9841. https://doi.org/10.3390/app12199841

Academic Editor: Alberto Villa

Received: 26 August 2022
Accepted: 26 September 2022
Published: 29 September 2022

Publisher's Note: MDPI stays neutral with regard to jurisdictional claims in published maps and institutional affiliations.

Copyright: © 2022 by the authors. Licensee MDPI, Basel, Switzerland. This article is an open access article distributed under the terms and conditions of the Creative Commons Attribution (CC BY) license (https://creativecommons.org/licenses/by/4.0/).

1. Introduction

Biomass compression molding pellet is a granular product with a certain diameter and density, which is compressed and formed by a biomass briquette machine from agricultural and forestry processing residues, such as sawdust and straw [1]. In the process of compressing loose materials into shaped particles with a certain shape and density, friction occurs by contact between the interior surface of the forming channel and biomass pellets [2]. The friction causes wear of the interior surface and eventually leads to the increase in the diameter *d* of the forming ring die, while the diameter *d* of the biomass pellets increases too. Therefore, there is a certain correlation between the interior surface morphology of the forming channel and the circular surface morphology of biomass pellets. Through the fractal parameter characterization of circular surface morphology of biomass pellet, the wear of the forming channel can be calculated and predicted quantitatively [3]. The rough surface is a component of the contact surface, and the geometrical characteristics of its surface have a direct impact on the contact characteristics. Establishing a proper and reasonable mathematical model of the rough surface is essential for establishing the contact model of the contact surface, and reflecting the variation law of contact characteristics [4].

As an important component of non-linear science, fractal theory was founded by the French mathematician Mandelbrot in the 1970s to describe the complexity of geometric space and the irregular characteristics of complex objects [5]. Fractal parameters are used to characterize biomass pellet [6], which can accurately describe the roughness morphology of its peripheral surface [7], and statistics the surface roughness morphology data. The fractal

parameter of biomass pellet has statistical property and scaling law [8]. For dense forming, the surface roughness of the pellet showed anisotropism [9] due to the combined effects of ring die spindle speed, biomass flow rate, and model parameters and shape [10,11]. However, on the time scale, the biomass forming pellet circumferential surface rough morphology is also statistically self-similar and scale-invariant [12]. Therefore, the fractal theory can be used to analyze the surface morphology of the biomass pellet circumference [13]. The morphology represents its quality, which is characterized by parameters such as diameter, roughness, molding density and hardness, and is ultimately used to study the frictional wear mechanism of the molded ring die.

The fractal dimension of a biomass pellet is a parameter to characterize its fractal characteristics, generally is a specific score, which reflects the complexity of pellets circumference [14,15]. Based on classical contact mechanics and Rowe adhesive wear, the fractal dimension value can be used to quantitatively calculate the frictional wear of biomass pellets and metal forming channel, with the model combination of fractal parameters, material property parameters, and machine compression parameters. Hertz classical contact mechanics theory states that local stresses are generated when two objects are in compressive contact [16], and the contact area is deformed. The distribution of contact stresses is localized when the contact area is strongly constrained [17]. Based on the microscopic image observation of the ring die wear position after the wear failure, and considering the hardness of the friction subs of the contacting objects, the wear is set to be mainly adhesive wear. The molecular "mechanical theory" of friction states that in engineering, there are both mechanical and molecular effects between two friction surfaces under the action of external forces [18]. Due to the roughness of the friction surface, the real area of contact on the friction surface occurs between the micro-convex body of the object, generating pressure, engagement, and intermolecular attraction [19,20]. The frictional force is the sum of the tangential resistance of all contacting micro-convex bodies on the friction surface due to mechanical and molecular attractive forces.

This paper selects biomass forming pellets formed by mixed wood chips as the research object, calculates the circumferential surface fractal dimension D of the forming pellets by the variance method, analyzes and studies its influencing factors. Based on this, the reconstruction of its surface morphology is studied to support further exploration of the wear pattern of key components of biomass molding machines.

2. Contact and Its Mechanical Analysis

It is known from the fractal theory that the forming surface of biomass forming ring die has fractal characteristics; therefore, the study of fractal parameters can establish the formula of sassafras force that characterizes the rough contact model of the surface between objects, and quantitatively calculate friction wear [21].

2.1. Friction Surface Contact State

Figure 1 [22] shows, let biomass forming machine forming ring die and biomass forming pellets for a pair of relative sliding friction sub-element O_1, O_2, and $z_1(x)$, $z_1(x)$ are the contour lines of mutual contact surfaces S_1, S_2 before contact deformation. Due to the finite scale characteristics of engineering applications, consider a certain micro-convex body pair i, which is in contact at a point at the moment t_0, will be displaced due to deformation after generating a relative sliding distance S in time Δt. The two dashed lines in the figure indicate that the two objects contour are not deformed, considering the elastic–plastic deformation, the original B_4,B_5 contact point moves to point B_2. Let A_i be the contact surface and let $\delta_1^{(i)}$, $\delta_2^{(i)}$ be its displacements, whose projections in the horizontal x and vertical z directions are $\delta_{x1}^{(i)}$, $\delta_{z1}^{(i)}$ and $\delta_{x2}^{(i)}$, $\delta_{z2}^{(i)}$. Due to the deformation and relative sliding action along the contact surface, the amount of change in the vertical distance between the two contact surfaces $\Delta h = S\tan\alpha - (\delta_{z1}^{(i)} + \delta_{z2}^{(i)}) = S\tan\alpha\text{-}\delta_{zi}$, where α is the inclination angle of the micro-contact surface. Since the area of a single micro-convex body micro-contact surface is small, the approximation takes the value $\tan\alpha = \partial_{z1}/\partial_{z1}$.

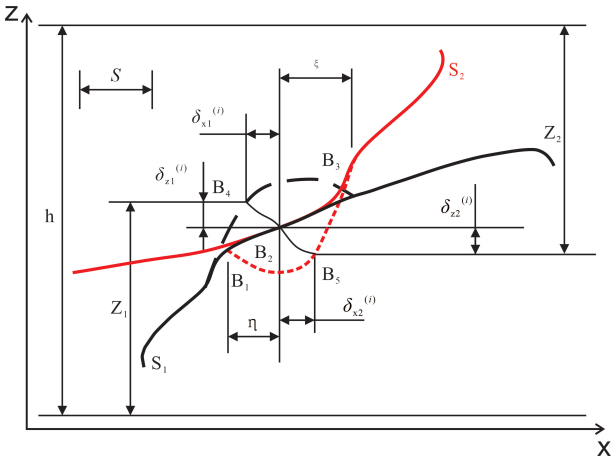

Figure 1. Contacting state of a pair of micro asperity after a relative sliding distances: s, relative sliding distance; h, distance between two reference planes; S_1, S_2, contact surface; Z_1, distance in the z-direction of the contact surface s1 before deformation; Z_2, distance in the z-direction of the contact surface S_2 before deformation;η, ξ, distance in x-direction of micro-convex body after deformation; ∂z, displacement in z-direction; ∂, displacement in x-direction.

set $V_x = \partial S/\partial t$, $V_z = \partial h/\partial t$. Derivative of both sides of the expression Δh with respect to time t, then substitute into $\tan\alpha = \partial_{z1}/\partial_{x1}$, and get Equation (1).

$$V_z = \frac{\partial S}{\partial t} = \frac{\partial h}{\partial t}\frac{\partial z_1}{\partial x_1} - \frac{\partial \delta_z^i}{\partial t} = V_x\frac{\partial z_1}{\partial x_1} - \frac{\partial \delta_z^i}{\partial t} \quad (1)$$

where V_x, V_z, relative sliding speed of the frictional sub-element along the x-direction and z-direction; ∂S, displacement in x-direction; ∂h, displacement in z-direction.

2.2. *Microscopic Contact Mechanics*

As shown in Figure 2, the mechanical deformation resistance q (perpendicular to the micro-contact surface) and molecular tangential resistance p (parallel to the micro-contact surface) in the contact region, the total contact pressure pt can be decomposed as $p_t^{(i)}(x,y,z) = p^{(i)}(x,y,z) + q^{(i)}(x,y,z)$.

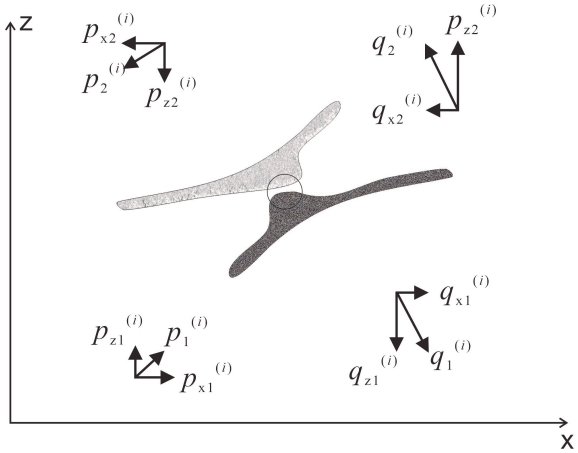

Figure 2. Force analysis of micro contacting surface; q, mechanical deformation resistance; p, molecular tangential resistance; q_{xn}, mechanical deformation resistance in x-direction; q_{zn}, mechanical deformation resistance in z-direction; p_{xn}, molecular tangential resistance in x-direction; p_{zn}, molecular tangential resistance in z-direction.

Considering only the contact surface motion in the xz plane and neglecting the y-direction motion and relative rotation, the following decompositions are obtained: $p_1^{(i)}$

$= p_{x1}^{(i)}x + p_{z1}^{(i)}z$, $p_2^{(i)} = -p_{x2}^{(i)}x - p_{z2}^{(i)}z$ and $q_1^{(i)} = q_{x1}^{(i)}x - q_{z1}^{(i)}z$, $q_2^{(i)} = -q_{x2}^{(i)}x + q_{z2}^{(i)}z$, where, $p_1^{(i)}$ and $p_2^{(i)}$, $q_1^{(i)}$ and $q_2^{(i)}$ are projected with equal magnitude and opposite direction in the corresponding directions. Then the slope at the contact point is related to the contact pressure as follows:

$$\frac{\partial z_1}{\partial x_1} = -\frac{\partial z_2}{\partial x_2} = \frac{q_{x1}^{(i)}}{q_{z1}^{(i)}} = \frac{q_{x2}^{(i)}}{q_{z2}^{(i)}} = \frac{p_{z1}^{(i)}}{p_{x1}^{(i)}} = \frac{p_{z2}^{(i)}}{p_{x2}^{(i)}} \tag{2}$$

where δ_{xn}, displacement at point n in z-direction; δ_{zn}, displacement at point n in z-direction; q_{xn}, mechanical deformation resistance at point n in x-direction; q_{zn}, mechanical deformation resistance at point n in z-direction; p_{xn}, molecular tangential resistance at point n in x-direction; p_{zn}, molecular tangential resistance at point n in z-direction.

Bringing Equation (2) into Equation (1) and integrating over the spatial contact surface A_i (i = 1,2,. . . ,n) yields

$$\sum_i \iiint_{A_i} \left[\frac{\partial \delta_z^{(i)}}{\partial t} p_{x1}^{(i)}\right] da_i = V_x \sum_i \iiint_{A_i} p_{z1}^{(i)} da_i - V_z \sum_i \iiint_{A_i} p_{x1}^{(i)} da_i \tag{3}$$

$$\sum_i \iiint_{A_i} \left[\frac{\partial \delta_z^{(i)}}{\partial t} q_{x1}^{(i)}\right] da_i = V_x \sum_i \iiint_{A_i} q_{z1}^{(i)} da_i - V_z \sum_i \iiint_{A_i} q_{x1}^{(i)} da_i \tag{4}$$

Integrating each side of Equation (1) over A_i to get the sum:

$$V_z \sum_i \iiint_{A_i} da_i = V_x \sum_i \iiint_{A_i} \frac{\partial z_1}{\partial x_1} da_i - \sum_i \iiint_{A_i} \frac{\partial \delta_z^{(i)}}{\partial t} da_i \tag{5}$$

The summation terms in Equation (5) are expressed in terms of A_0, A_r (the true contact area of the two contact surfaces), and E_0 (the time rate of change of the z-directional deformation), respectively:

$$A_0 = \sum_i \iiint_{A_i} \frac{\partial z_1}{\partial x_1} da_i \quad A_r = \sum_i \iiint_{A_i} da_i \quad E_0 = \sum_i \iiint_{A_i} \frac{\partial \delta_z^{(i)}}{\partial t} da_i \tag{6}$$

Set the components of mechanical deformation resistance and molecular tangential resistance in z and x direction on the whole contact surface be T_{z1} , T_{x1} and R_{z1}, R_{x1}, respectively. Let the left side of Equations (3) and (4) as $W(1)$, $W(2)$, respectively, and bring them into Equation (5) to get V_z [T_{z1} /$W(1) - A_r/E_0$] + $V_x[A_0/E_0 - T_{x1}/W(1)]$ = 0, $V_z R_{x1}[/W(2) - A_r/E_0] + V_x[A_0/E_0 - R_{z1}/W(2)] = 0$. Set $A_0 = cA_r$,it is known that $0 < c < 1$, then $T_{x1} = (A_0/A_r\ T_{x1} = cT_{z1}\ R_{z1} = (A_0/A_r\ R_{x1} = cR_{x1}$. If the shear strength of the molding die hole material is ι and A_{rp} is the plastic contact area,then $R_{x1} = \iota\ A_{rp}$, and let the normal load between the contact surface of the molding die hole and the molding particles be F_N, then $F_N = R_{z1} + T_{z1}$, then the frictional force between the contact surface of the molding die hole and the molding particles can be expressed as $F = R_{x1} + T_{x1} = cF_N + (1 - c^2)\ R_{x1} = cF_N + (1 - c^2)\ \iota\ A_{rp}$.

The rough surface self-affine fractal features, therefore based on the rough surface fractal characterization and Hertz theory [21], then get the equation as follows:

$$\begin{aligned} A_{rp} &= \left(\frac{D}{2-D}\right)^{(2-D)/2} \psi^{(2-D)^2/4} A_r^{D/2} a_c^{(2-D)/2} \\ &= \left(\frac{D}{2-D}\right)^{(2-D)/2} \psi^{(2-D)^2/4} A_r^{D/2} G^2 \left[\frac{\pi E^2}{225\sigma_y^2}\right]^{(2-D)/2(D-1)} \end{aligned} \tag{7}$$

where D is the fractal dimension of the surface profile; Ψ satisfies the transcendental equation: $\Psi^{(2-D)/2} - \left(1+\Psi^{-D/2}\right)^{-(2-D)/D} = (2-D)/D$; a_c, the critical area at the micro-contact point when plastic change occurs; G,the fractal dimensional characteristic factor reflecting the magnitude of the surface profile of the die hole; σ_y, the yield strength of the molded particle material; E,the composite elastic modulus.

Let the unit expansion force given by the ring die to the molding particles is F_0, the contact area is A_a, the length of the molding particles is l_γ, and the minimum contact circumference is d. Then, $F_N = F_0 A_a = dF_0 l_\gamma$, and the fractal expression of the contact surface friction between the die hole and the molding particles based on the fractal dimension can be obtained by substituting into Equation (6) and above.

$$F = cF_0 l_r d + \left(1-c^2\right)\tau\psi^{(2-D)^2/4} G^{2-D} A_r^{D/2} \left(\frac{D}{2-D}\left[\frac{\pi E^2}{225\sigma_y^2}\right]^{1/(D-1)}\right)^{(2-D)/2} \tag{8}$$

2.3. Fractal Modeling of Circumferential Surface Morphology of Pellets

Biomass forming pellets with a certain moisture content and particle size have a certain shape and density. The surface structure of the circumference of the formed pellets has obvious self-similarity and unsmoothness, so the fractal theory can be used to describe and characterize the surface morphology of the circumference of the biomass formed pellets. The W-M fractal function is an ideal curve that is continuous, non-differentiable and has self-affine fractal characteristics everywhere, which can simulate the engineering surface contours such as the circumferential surface of the formed particles. It is described as follows [22]:

$$Z(x) = G^{D-1} \sum_{n=\omega_L}^{\omega_U} \frac{\cos(2\pi\gamma^n x)}{\gamma^{(2-D)n}} \tag{9}$$

where $Z(x)$,the height of the circumferential surface profile of the pellet;x, a contour measurement coordinate; G, the characteristic scale factor of the surface profile of the formed pellet, m, and $G^{D-1} = 2\sigma(\omega_L\omega_U)^{2-D}\left(\frac{2-D}{\omega_U^{4-2D}-\omega_L^{4-2D}}\right)^{1/2}$, the standard deviation σ is taken as 0.05; γ^n, contour spatial frequency; γ takes 1.5,n is an integer; ω_L is truncated low frequency upper limit of surface profile, $\omega_L = 1/L$, (L,the surface profile sampling length, takes 0.004m); ω_U, truncated HF upper limit of contour, $\omega_U = 1/2\sigma$, (σ contour resolution, takes 0.001).

3. Materials and Methods

3.1. Materials and Instruments

Biomass pellets (Figure 3) used in these experiments were manufactured in Hohhot city, Inner Mongolia Autonomous Region, China, using a mix of pine, poplar and corn straw. The raw materials moisture content of about 11% and granularity of about 1∼3 mm. Biomass pellets were made by biomass ring-die briquetting machine (Figure 4), which is designed and manufactured by the authors, with process parameters: die rotational speed of 60 rpm, die channel diameter of 6 cm and 8cm, corresponding die channel depth of 29 cm and 40 cm.

The density of pellets obtained after densification is about 1.05∼1.31 g cm^{-3}.



(a) (b)

Figure 3. Biomass pellet: (**a**) *d*0 = 6 mm, (**b**) *d*0 = 8 mm.



Figure 4. Biomass ring-die briquetting machine.

Test instruments and equipment: HITACHI S-4800 scanning electron microscope, JB-8C surface roughness meter of Guangjing Precision Instrument Co. DHS-10A moisture content tester, HLX-D surface hardness tester, vernier caliper, OHAUS AR224CN electronic balance, standard inspection sieve with 3 mm mesh diameter (GB/T 6003.1-2012).

3.2. Surface Contour Fractal Dimension Determination

As a modern mathematical tool to depict non-linear and irregular morphology from a geometric point of view, fractal theory determines the fractal dimension as a key problem to characterize the rough morphology of the circumferential surface of biomass pellets by fractal dimension. For the study of the circumferential surface morphology of wood chip forming pellets, the variance method is selected for the calculation of fractal dimension for better linearity [23]. Let the difference between the maximum and minimum values of the surface profile in the *i*th box is *Hi*, if *r* is small to the limit, the value of *Hi* approximates the curve length. Therefore, the expression of the equivalent measure $V(r)$ is as follows.

$$V(r) = \frac{\sum rH_i}{r^2} = \frac{\sum H_i}{r} \tag{10}$$

By making a linear regression analysis of $V(r)$ and r in double logarithmic coordinates, the fractal dimension of the contour can be obtained from the slope of the line α.

$$D = 2 - \alpha \tag{11}$$

4. Results and Discussion

The measurement and calculation of the actual diameter d, density ρ, moisture content of the formed pellets and the measurement of the hardness HD value on the surface of the pellets using a hardness tester were carried out for the pellets formed with a biomass ring die forming machine with die hole diameters of 6 mm and 8 mm, respectively, and extruded mixed wood chip materials; using the surface roughness meter to measure the surface roughness parameter *R*a value of the circumference of the corresponding pellets, and get

its surface fractal profile curve; calculation of the fractal dimension D of the circumferential surface morphology of biomass-forming particles using the variance method.

Figure 5 shows the surface roughness profile of the circumference of a sample of formed pellet with diameter of 8 mm, at an arithmetic mean roughness parameter Ra = 2.05 μm, visualize the relationship between rough shape and Ra.

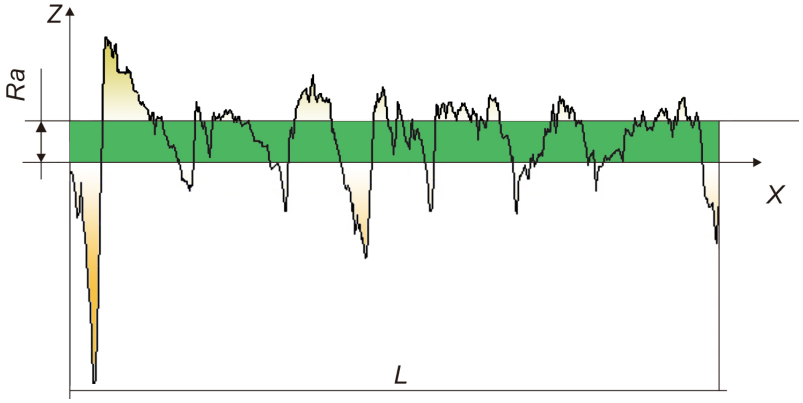

Figure 5. Surface roughness of the molding particle (Ra = 2.05 μm).

4.1. Influencing Factors on Fractal Parameters of Biomass Pellet

The results of the data obtained are shown in Table 1.

Table 1. Analysis of influencing factors on fractal parameters of biomass pellet.

Sample	$d0$ = 6 mm					$d0$ = 8 mm				
	d (mm)	ρ (g cm^{-3})	Ra (μm)	HD	D	d (mm)	ρ (g cm^{-3})	Ra (μm)	HD	D
1	6.04	1.351	1.39	64.44	1.806	8.12	1.502	0.7	66.05	1.914
2	6.08	1.304	1.25	63.2	1.82	8.26	1.483	0.9	66	1.789
3	6.11	1.298	1.47	62.73	1.649	8.32	1.452	0.94	65.29	1.664
4	6.31	1.235	2.18	63	1.69	8.37	1.398	1.05	62.02	1.672
5	6.46	1.181	2.01	60.28	1.61	8.38	1.36	1.14	60.9	1.635
6	6.84	1.135	2.44	50.63	1.6	8.48	1.351	1.77	58	1.655
7	7	1.108	2.66	43.17	1.578	8.55	1.267	1.91	56.17	1.628
8	7.24	1.076	2.23	48	1.431	8.58	1.204	2.22	55.01	1.588
9	7.41	1.042	2.84	45.83	1.536	8.76	1.285	2.93	54.04	1.476
10	7.65	1.025	2.99	41.2	1.494	8.98	1.269	3.31	55.03	1.43

Table 1 indicates the actual diameter d values of the compressed biomass forming pellets under the ring die forming die hole $d0$ = 6 mm and 8 mm, as well as their corresponding density ρ, surface roughness Ra, and surface hardness HD, while the surface morphology is calculated using the variational method, and the fractal dimension D values corresponding to the surface morphological characteristics are derived using Equation (10). For $d0$ = 6 mm, the fractal dimension of the particles ranged from 1.494 to 1.806, but mostly concentrated around 1.6; for $d0$ = 8 mm, the fractal dimension ranged from 1.430 to 1.914, but mostly concentrated around 1.6, indicating that the fractal dimension of biomass pellets are an isotropic and at the same time self-similar [24,25].

The data in Table 1 also allow to derive the fractal dimension D as a function of pellet forming diameter d (Figure 6), density ρ (Figure 7), hardness HD (Figure 8), and roughness Ra (Figure 9).

Figure 6 Relationship between d and D. The analysis in Figure 5 shows that the fractal dimension D tends to decrease as the diameter d of biomass pellets increases. This is mainly because as the diameter of the formed pellets increases, the surface roughness becomes rougher, and the D value calculated by the variance method becomes smaller. The reason why the molding diameter d of wood pellets is larger than the diameter $d0$ of the forming channel is due to the friction caused to the forming channel by the wood chip materials during the compression molding process. Biomass material comes into periodic contact

with protruding parts of the die hole surface or ploughs under cyclic loading, and fatigue spalling of the metal material in this area due to repeated plastic hardening [1]. Thus, the diameter of the die hole becomes larger after wearing, the more serious the forming die hole wear, the diameter of forming pellets also increases.

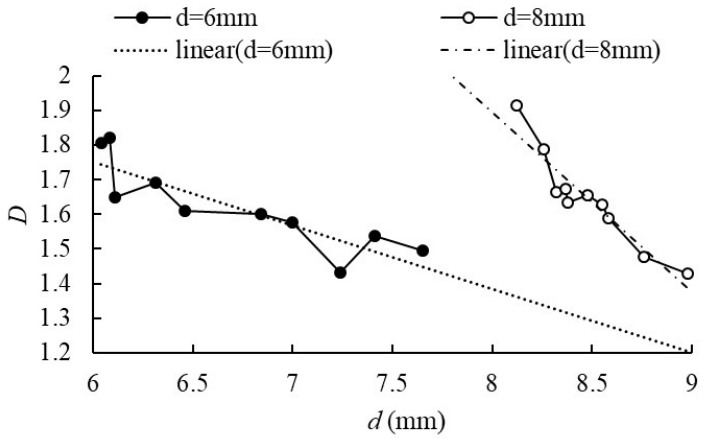

Figure 6. Relationship between d and *D*.

From the Figure 7, it can be seen that the fractal dimension *D* tends to increase as the density ρ of biomass pellets increases. This is mainly because the greater the density ρ of the pellets, the tighter the bonding between the pellets, the better the denseness, and, therefore, the smoother the surface of the pellets, and, therefore, the greater the *D* value calculated by the variance method.

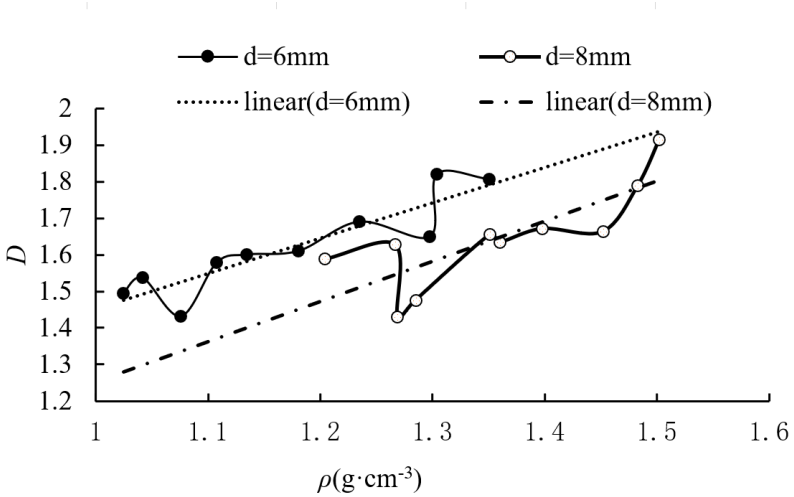

Figure 7. Relationship between ρ and *D*.

Figure 8 shows that the fractal dimension *D* tends to decrease as the surface roughness parameter *R*a of biomass pellet increases. This is mainly because the larger the *R*a value of the surface roughness parameter of the pellet, the more uneven the surface morphology of the pellet is, and the smaller the *D* value calculated by the variance method. The surface with small Ra is generally more complex and has a deeper self-similar fine structure than the surface with large *R*a, so the friction subsurface becomes polished, the surface morphology becomes fine and complex, the fractal characteristics are more obvious, and the fractal dimension becomes progressively larger [26].

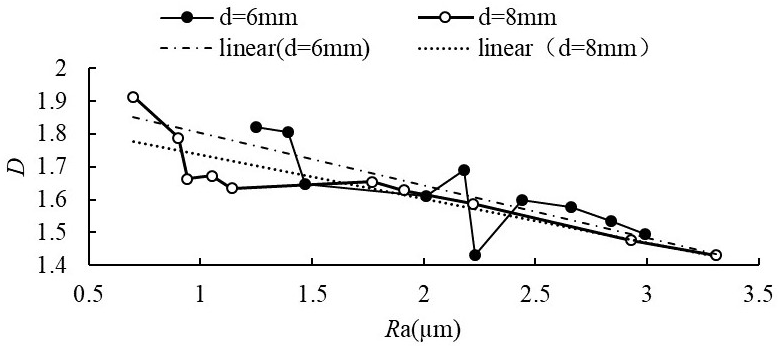

Figure 8. Relationship between *R*a and *D*.

From the analysis of Figure 9, it can be seen that the fractal dimension *D* tends to rise as the hardness of biomass forming particles HD increases, which is mainly because the higher the hardness of the pellet surface indicates that the denseness of the pellet is also better and the surface is smoother, therefore, the *D* value obtained by the variance method is also larger.

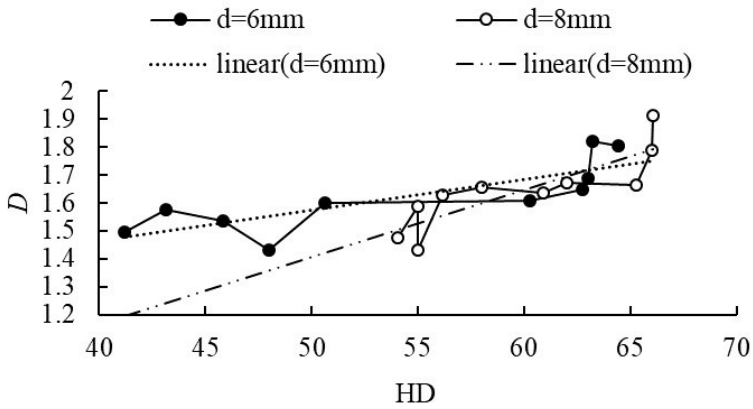

Figure 9. Relationship between HD and *D*.

4.2. Electron Microscope Observation of the Rough Surface Shape of the Circumference of the Pellets

The surface and the internal void structure of pellet can be shown more visually and clearly using scanning electron microscopy [27,28]. Figures 10 and 11 show the electron microscope scans of the rough surface morphology of the circumference of the formed pellets at a magnification of 500 times when using biomass forming machines with forming die holes of ϕ 6 mm and ϕ 8 mm, respectively, where the dark area indicates a relatively smooth surface and the white linear area is indicating the rough cracked surface area.

Using Python to calculate the percentage of white rough area, the area of white area on the surface of the molded pellet represented by 9-a plot (d = 6.08 mm, D = 1.820) is 6.08%, indicating that the more smooth the surface of the pellet is relatively; while the area of white area on the surface of the pellet represented by 9-c plot (d = 7.41 mm, D = 1.536) is 16.3%, indicating that that the surface is relatively rougher. From Figure 10, it is also clear that the white area on the surface of the pellet in the 10-a plot (d = 8.26 mm, D = 1.789) is 6.85%, which indicates that the surface of the pellet is relatively smoother, while the white area on the surface of the pellet in the 10-c plot (d = 8.76 mm, D = 1.476) is 19.6%, which indicates that the surface of the pellet is relatively rougher.

It can be synthesized that with the increase in the molding pellet diameter, the rougher the surface morphology of the pellet, the larger the surface roughness value, and the surface fractal dimension *D* becomes smaller subsequently. Electron microscopy experiments proved that measuring the fractal dimension of the particle surface using SEM technique is an effective way for quantitative analysis [29].

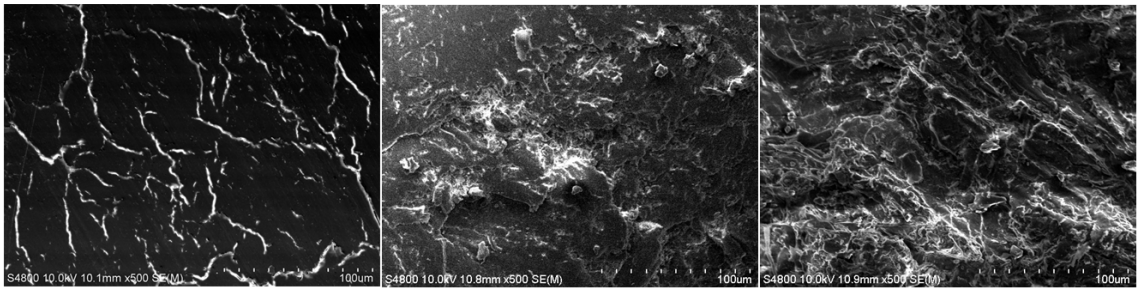

(a) **(b)** **(c)**

Figure 10. Circular surface morphology of ϕ 6 mm biomass pellet: (**a**) d = 6.08 mm, D = 1.820, (**b**) d = 6.84 mm, D = 1.6, (**c**) d = 7.41 mm, D = 1.536.

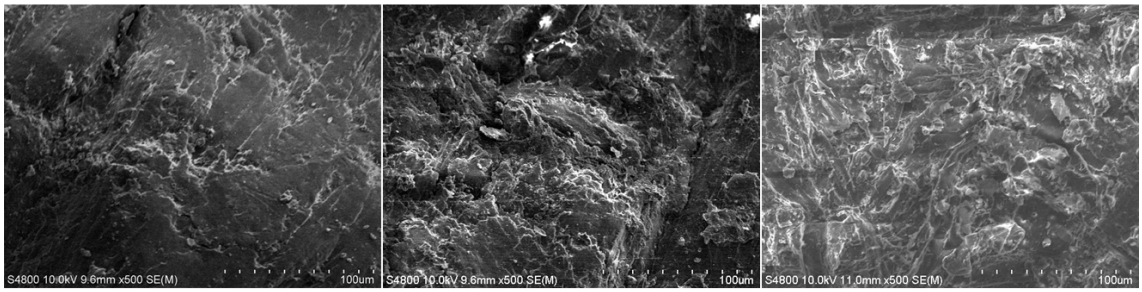

(a) **(b)** **(c)**

Figure 11. Circular surface morphology of ϕ 8mm biomass pellet: (**a**) d = 8.26 mm, D = 1.789, (**b**) d = 8.58 mm, D = 1.588, (**c**) d = 8.76 mm, D = 1.476.

4.3. Analysis of Test Results

The above analysis shows that as the diameter d of the pellets increases, the density ρ tends to decrease, the roughness Ra tends to increase, the hardness HD tends to decrease, and the fractal dimension D tends to decrease. This is mainly because, with the increase in pellet diameter d, it means that the wear of the ring die forming die hole intensifies, the roughness value of the inner surface of the forming die hole increases, and the aspect ratio of the forming die hole ($h/d0$) decreases, which causes the quality of the pellets to decrease, i.e., the dense degree decreases, so that the density of the pellets ρ decreases, the surface roughness Ra of the pellets decreases, and the pellets become relatively loose, so that the surface hardness HD value of the f pellets decreases. Therefore, the relationship between the calculated fractal dimension D value and the diameter of pellets d, can be known, and the size of the fractal dimension D and the trend of change can be used to analyze and judge the quality of biomass pellets, and at the same time, the wear condition of the forming mold hole of biomass forming machine can be reflected to predict the life of ring mold.

5. Conclusions

In this paper, mixed biomass (moisture content about 11%, granularity 1∼3 mm; density 1.05∼1.31 g·cm^{-3}) was compressed into formed pellets by a biomass ring mold machine (mold hole d0 of 6 and 8 mm), and the rough surface morphology parameters Ra of the circumference of the formed pellets were collected, their particle diameters d, density ρ and hardness HD were measured, and their corresponding fractal dimensions D were calculated to analyze their on the circumferential fractal dimension of the pellet surface, and then scanned its surface morphology by electron microscopy to obtain the following conclusions.

1. The fractal dimension D can characterize the rough morphological features of the circumferential surface of biomass pellets;

2. As the diameter d of the formed particles increases, the density ρ tends to decrease, the roughness Ra tends to increase, the hardness HD tends to decrease, and the fractal dimension D tends to decrease;
3. The magnitude and trend of the fractal dimension D value can be used to analyze and judge the quality of biomass forming pellets and deduce the wear condition of the forming mold hole of biomass forming machine.

Author Contributions: Conceptualization, J.Z., X.D., Z.Y.; methodology, J.Z., X.D.; software, J.Z.; validation, J.Z., X.D.; formal analysis, J.Z., X.D.; investigation, J.Z., X.D., Z.Y.; resources, J.Z.; data curation, J.Z, W.G.; writing—original draft preparation, J.Z., X.D., Z.Y.; writing—review and editing, J.Z.; visualization, Y.G., W.G., X.C.; supervision, Z.Y.; project administration, X.D., Z.Y.; funding acquisition, X.D., Z.Y. All authors have read and agreed to the published version of the manuscript.

Funding: National Natural Science Foundation of China (NSFC) Project (51766016; 51865047; 31960365).

Institutional Review Board Statement: Not applicable.

Informed Consent Statement: Not applicable.

Data Availability Statement: Data available within the article.

Conflicts of Interest: The authors declare no conflicts of interest.

References

1. Xia, X.; Sun, Y.; Wu, K.; Jiang, Q. Wear mechanism of ring die for straw briquetting machine. *Trans. CSAE* **2014**, *30*, 32–38.
2. Holm J.K.; Stelte W.; Posselt D.;Ahrenfeldt, J.; Henriksen, U.B. Optimization of a multiparameter model for biomass pelletization to investigate temperature dependence and to facilitate fast testing of pelletization behavior. *Energy Fuels* **2011**, *25*, 3706–3711.
3. Jiang, Q.; Wu, K.; Sun, Y.; Xia, X. Wear mechanism analysis of ring die of pellet mill. *Trans. CSAE* **2013**, *29*, 42–44.
4. Buczkowski, R.; Kleiber, M. Statistical Models of Rough Surfaces for Finite Element 3D-Contact Analysis. *Arch. Comput. Methods Eng.* **2009**, *16*, 399–424.
5. Falconer, K. *Fractal Geometry: Mathematical Foundation Sand Applications*; John Wiley: New York, NY, USA, 1989; pp. 25–68.
6. Ghanbarian, B.; Daigle, H. Fractal dimension of soil fragment mass-size distribution: A critical analysis. *Geoderma* **2015**, *103*, 245–246.
7. Xiao, Y.; Wu, L.; Luo, J.; Zhou, L. Mechanical response of thin hard coatings under indentation considering rough surface and residual stress. *Diamond Related Mater.* **2020**, *108*, 107991.
8. Li, Z.; Wang, P.; Liu, P.; Gao, Y.; Wang, H. Fatigue life analysis of key components of ring molding machine based on fluid-solid coupling. *J. For. Eng.* **2020**, *5*, 122–128.
9. Nieslony, P.; Krolczyk, G.M.; Wojciechowski, S.; Chudy, R.; Zak, K.; Maruda, R.W. Surface quality and topographic inspection of variable compliance part after precise turning. *Appl. Surf. Sci.* **2018**, *434*, 91–101.
10. Kamperidou, V. Quality Analysis of Commercially Available Wood Pellets and Correlations between Pellets Characteristics. *Energies* **2022**, *15*, 2865.
11. Huo, L.L.; Zhao, L.X.; Hao, Y.H.; Meng, H.B.; Yao, Z.L.; Liu, Z.; Liu, T.L.; Yuan, Y.W. Quality standard system of densified biomass fuels at home and abroad. *Trans. Chin. Soc. Agric. Eng.* **2020**, *36*, 245–254.
12. Yan, W.G. *Research of Biomass Shaping with Open Mold in Natural Temperature*; Beijing Forestry University: Beijing, China, 2011.
13. Yang, Y.C.; Peng, R.D.; Zhou, H.W. Computation of fractal dimension for digital image in a 3D space. *J. China Univ. Min. Technol.* **2009**, *19*, 107–114.
14. Wen, S.Z.; Huang, P. *Principle of Tribology*; Tsinghua University Press: Beijing, China, 2002; pp. 120–150.
15. Weng S.; Chen J.; Zhou J.; Lin X. Wear Mechanism Analysis in Subsurface for Al Substrate Scraped by Abrasive Particle from Atomic Simulation. *Materials Reports,* **2022**, *36(1)*, 20110027.
16. Tan, W.B.; Lan, G.S.; Zhang, X.L.; Sun W.; Wen S.; cHEN y. Modeling and simulation analysis of elliptic-plastic normal contact stiffness of joint surface based on anisotropic fractal theory. *Chin. J. Solid Mech.* **2021**, *42*, 63–76.
17. Liu, Y.; Xia, T.; Chen, Z.Y.; Yan G. Presentation and development of statistical contact model for rough surfaces. *Tribology* **2020**, *40*, 395–406.
18. Yang, X.; Robert, L.J. Statistical Models of Nearly Complete Elastic Rough Surface Contact-Comparison with Numerical Solutions. *Tribol. Int.* **2017**, *105*, 274–291.
19. Huang, Y.K. *Study on Contact Model of Rough Surface with Real Topography*; North University of China: Taiyuan, China, 2020; pp. 98–100.
20. Huang, S.Z.; Liu, J.; Shen, H.M. Numerical study of the effect of initial roughness on tangential fretting behavior. *J. Sichuan Univ. Sci. Eng. (Nat. Sci. Ed.)* **2020**, *33*, 13–18.
21. Valentin, L.P.; Li, Q.; Luo, J.B. *The Principle and Application of Contact Mechanics and Tribology*, 2nd ed.; Tsinghua University Press: Beijing, China, 2019.

22. Ge, S.R.; Zhu, H. *Fractal of Tribology Machinery*; Industry Press: Beijing, China, 2005.
23. Li, Y.; Peng, J.; Zhang, L.; Zhou, J.; Huang, C.; Lian, M. Quantitative evaluation of impact cracks near the borehole based on 2D image analysis and fractal theory. *Geothermics* **2022**, *100*, 102335.
24. Denghui, M.A.; Huayan, Y.A.O.; Xinzhi, W.A.N.G.; Yinghui, L.Ü. Particle shape characteristics of coral sands. *J. Eng. Geol.* **2021**, *29*, 1452–1459.
25. Shi, X.; Wang, W.; Liu, K.;Chen R.; Yang L.; Feng S.; Construction and contact analysis of micro-random rough surface contact finite element mode. *Lubr. Eng.* **2020**, *45*, 25–29.
26. Panagouli, O.K. Effects of multi-scale structure and fractal dimension on the friction mechanism in rough surfaces under horizontal dynamic excitation.*Appl. Fractals* **2017**, *89*, 197–222.
27. Deng, Y.J.; Peng, L.F.; Lai, X.M.; Fu, M.W.; Lin, Z.Q. Constitutive modeling of size effect on deformation behaviors of amorphous polymers in micro-scaled deformation.*Appl. Int. J. Plast.* **2017**, *89*, 197–222.
28. Chen, J.; Ding, X.; Zhang, W.; Yan, R.; Sun, B. Fractal prediction model for the thermo-elastic normal contact stiffness of frictional interfaces in dry gas seals. *Appl. J. Vib. Shock* **2020**, *39*, 257–263.
29. Bellucci, S.; Bolesta, I.; Karbovnyk, I.; Hrytskiv, R.; Fafilek, G.; Popov, A.I. Microstructure of Ag2BI4 (B = Ag, Cd) superionics studied by SEM, impedance spectroscopy and fractal dimension analysis. *Appl. J. Phys. Condensed Matter* **2008**, *20*, 474211.